

Search for Narrow Nucleon Resonance in $\gamma p \rightarrow \eta p$

A.V. Anisovich^{a,b}, E. Klempt^b, V. Kuznetsov^{c,d}, V.A. Nikonov^{a,b}, M.V. Polyakov^{a,d,*}, A.V. Sarantsev^{a,b}, U. Thoma^b

^a*Petersburg Nuclear Physics Institute, Gatchina, St.Petersburg 188300, Russia*

^b*Helmholtz-Institut für Strahlen- u. Kernphysik, Universität Bonn, Germany*

^c*Institute for Nuclear Research, 117312, Moscow, Russia*

^d*Institut für Theoretische Physik II, Ruhr-Universität Bochum, D-44780 Bochum, Germany*

Abstract

Results of a partial wave analysis of new high-statistics data on $\gamma p \rightarrow p\eta$ from MAMI are presented. A fit using known broad resonances and only standard background amplitudes can not describe the relatively narrow peaking structure in the cross section in the mass region of 1660-1750 MeV which follows a minimum. An improved description of the data can be reached by either assuming the existence of a narrow resonance at a mass of about 1700 MeV with small photo-coupling or by a threshold effect. In the latter case the observed structure is explained by a strong (resonant or non-resonant) $\gamma p \rightarrow \omega p$ coupling in the S_{11} partial wave. When the beam asymmetry data, published by part of the GRAAL collaboration, are included in the fit, the solution with a narrow P_{11} state is slightly preferred. In that fit, mass and width of the hypothetical resonance are determined to $M \sim 1694$ MeV and $\Gamma \sim 40$ MeV, respectively, and the photo-coupling to $\sqrt{\text{Br}_{\eta N}} A_{1/2}^p \sim 2.6 \cdot 10^{-3} \text{ GeV}^{-1/2}$. High precision measurements of the target asymmetry and F -observable are mandatory to establish the possible existence of such a narrow state and to provide the necessary information to define which partial wave is responsible for the structure observed in the data.

Keywords:

All nucleon resonances listed in the Review of Particle Properties [1] have rather large widths of $\Gamma \gtrsim 100$ MeV. Such widths of nucleon resonances are natural for the constituent quark model picture of baryons (see the recent review of the baryon spectroscopy and quark model ideas in Ref. [2]). The chiral quark soliton model (χ QSM) [3] challenges the constituent quark model picture of nucleon resonances. Here, a SU(3) anti-decuplet of light and narrow baryons is predicted. In particular, the existence of the P_{11} ($J^P = \frac{1}{2}^+$) nucleon state, much narrower (≤ 40 MeV) than normal nucleon excitations of similar mass, was predicted [3, 4, 5, 6].

Ref. [8] predicts that a nucleon resonance from the anti-decuplet is excited predominantly by photons off neutrons, whereas its photo-excitation off protons is strongly suppressed. Such a pattern, if observed, provides an imprint of the exotic nature of a state. A partial wave analysis (PWA) of data on elastic πN scattering showed that the existing data on πN scattering can tolerate a narrow P_{11} resonance at a mass around 1680 MeV

if its πN partial decay width is below 0.5 MeV [5]. Such a suppression of the πN decay channel is predicted in χ QSM [3, 5, 6]. The fact that the excitation of the anti-decuplet nucleon in πN and γp collisions is expected to be very weak makes the search of the anti-decuplet nucleon a challenging task. Firstly, one needs high precision and high resolution data¹. Secondly, a detailed PWA of the data needs to be performed to reveal a weak resonance signal. In contrast to γp reactions, the signal of the anti-decuplet nucleon is expected to be rather sizable in γn collisions [8].

Recently a peak structure has been observed in η -photoproduction of the neutron, at $W \sim 1680$ MeV, by GRAAL [9, 10], CBELSA/TAPS [11, 12], LNS [13], and Crystal Ball/TAPS [14]. Various explanations for the structure have been proposed in the literature. The structure can be produced by interference effects e.g. in the S_{11} -wave as suggested in [15]. In [16] the narrow structure was explained in terms of coupled channel effects related to the $S_{11}(1650)$ and the $P_{11}(1710)$ -resonances. In the K-matrix coupled channel approach

*Corresponding author

Email addresses: maxim.polyakov@tp2.rub.de (M.V. Polyakov), andsar@hiskp.uni-bonn.de (A.V. Sarantsev)

¹See [7] where the required precision and resolution of the πN scattering data to reveal the anti-decuplet nucleon is discussed.

of [17] interference between $S_{11}(1535)$, $S_{11}(1650)$, $P_{11}(1710)$, and $P_{13}(1710)$ leads to the peak-like structure. A similar explanation but with an additional contribution from a rather narrow $D_{13}(1700)$ state was suggested in [18]. In [19] the effect was explained by interference of the two S_{11} states and a strong cusp effect at the $K\Lambda$ and $K\Sigma$ thresholds.

A very different interpretation is provided in [20, 21]. It was shown that in η -photoproduction of the neutron the signal can be described by the contribution of a narrow resonance. In γn collisions (with non-suppressed exit channels such as ηn , γn , $K_S\Lambda$, etc.) the anti-decuplet state should be seen as a clear narrow peak in the cross section [8].

Recently [22], quasi-free Compton scattering on the neutron in the energy range of $E_\gamma = 750 - 1500$ MeV was studied. The data indicate the existence of a narrow ($\Gamma \sim 35$ MeV) peak at $W \sim 1685$ MeV. The peak is absent in the Compton scattering off protons as well as in the reactions $\gamma n \rightarrow \pi^0 n$ and $\gamma p \rightarrow \pi^0 p$. The latter observation implies that the putative narrow resonance should have a very small πN partial width, in agreement with the modified PWA of Ref. [5] and with theoretical expectations for the anti-decuplet nucleon [3, 4, 5, 6].

If the peak at 1680 MeV would be due to narrow nucleon resonance, it should as well contribute to the γp channel. However, if it is related to the antidecuplet state, its contribution is predicted to be considerably suppressed. Possibly, it can nevertheless be seen in observables exploiting its interference with a strong smoothly varying background. The corresponding signal would then not necessarily look like a peak but may appear rather as a structure oscillating with energy, or as a dip.

A first search of the putative anti-decuplet nucleon in $\gamma p \rightarrow \eta p$ process was performed in Refs. [23, 24]. It was found that the beam asymmetry Σ , published by part of the GRAAL collaboration, exhibits a structure around $W \sim 1685$ MeV. That structure looks like a peak at forward angles which develops more into an oscillating structure at larger scattering angles. Such a behavior may occur by interference of a narrow resonance with a smooth background. The observed structure was identified in Refs. [23, 24] with the contribution of a resonance with mass $M \sim 1685$ MeV, narrow width of $\Gamma \leq 25$ MeV, and small photo-coupling of $\sqrt{\text{Br}_{\eta N} A_{1/2}^p} \sim (1 - 2) \cdot 10^{-3} \text{ GeV}^{-1/2}$.

Recently, the Crystal Ball Collaboration at MAMI published high precision data on η photoproduction on the free proton [25]. The cross section was measured in fine steps in photon energy. The measured cross section exhibits a minimum at masses around ≈ 1680 MeV fol-

lowed by a slight maximum around 1700 MeV. The best fit to the data was achieved with a new version of SAID (GE09) [25]. The authors interpret the fit as evidence against the existence of a narrow bump at 1680 MeV in this reaction. However, inspection of their fit reveals a systematic excess of data above their fit curves in the 1710 – 1730 MeV region.

In [26] the data of Ref. [25] were interpreted as indication for a nucleon resonance with mass of $M \sim 1685$ MeV, a narrow width of $\Gamma \leq 50$ MeV, and a small resonance photo-coupling in the range of $\sqrt{\text{Br}_{\eta N} A_{1/2}^p} \sim (0.3 - 3) \cdot 10^{-3} \text{ GeV}^{-1/2}$. In this case no PWA of the data was done as needed to decide whether or not a resonance occurs in a certain partial wave.

In this Letter we report on a PWA of the new MAMI data [25] which aims to trace the physical origin of the small deviation between data and the SAID (GE09) fit. The MAMI data are incorporated into the large data base on pion- and photo-induced reactions which is exploited in the Bonn-Gatchina coupled-channel analysis. PWA methods are described in detail in [27, 28, 29, 30, 31], a list of data used in the most recent analysis is given in [32]. In the latter work, two main solutions, BG2010-01 and BG2010-02, were found. These solutions have very close parameters for the resonances below 1800 MeV but differ in couplings and pole positions for higher-mass states. The description of the observables, multipoles and πN transition amplitudes with these solutions can be downloaded from [33].

Both solutions show small but systematic deviations from the data of Ref. [25], from the threshold up to 1750 MeV. At higher masses, the new data seem to be compatible with the Crystal Barrel measurements [35]. However, the latter data are presented in larger energy bins. Using this data, we re-optimized the parameters of the fit-solutions. In the present fit we included MAMI data with effective errors by adding quadratically statistic and systematic errors.

Only a small redefinition of parameters was required to obtain a rather good overall description of the MAMI data for both solutions (BG2010-01 and BG2010-02) with a χ^2 per data point of $\chi^2/N_{\text{dat}} = 1.21$. However, in the 1660 – 1750 MeV mass interval and, especially, above 1700 MeV, the solutions still have statistically significant deviations between data and fit. In this interval, $\chi^2/N_{\text{dat}} = 1.46$ is considerably larger than in other energy intervals. This is illustrated in Fig. 1 for the differential cross sections and in Fig 2 for the total cross section. The differential cross section is not described well in the angular region $0 < \cos \Theta < 0.5$ for the energy bins at 1667, 1671 and 1700 to 1730 MeV.

Table 1: The description of the MAMI [25] and beam asymmetry data [23, 24]. For the P_{11} narrow state two solutions with positive $P_{11}(+)$ and negative $P_{11}(-)$ interferences are given. The $\chi^2_{\text{sel}}/N_{\text{dat}}$ corresponds to the χ^2 per point for the mass region 1660-1750 MeV. The $\chi^2_{\Sigma}/N_{\text{dat}}$ corresponds to the χ^2 per point for the beam asymmetry data from [23, 24] and from [36]. Masses and widths are in MeV units. The photocouplings are in units of $10^{-3} \text{ GeV}^{-1/2}$.

Resonance	Mass	Γ_{tot}	$\sqrt{\text{Br}_{\eta N} A_{1/2}^P}$	$\sqrt{\text{Br}_{\eta N} A_{3/2}^P}$	$\chi^2_{\text{tot}}/N_{\text{dat}}$	$\chi^2_{\text{sel}}/N_{\text{dat}}$	$\chi^2_{\Sigma}/N_{\text{dat}}$ [23, 24]	$\chi^2_{\Sigma}/N_{\text{dat}}$ [36]
no res.	-	-	-	-	1.21	1.46	1.52	1.40
$P_{11}(+)$	1719	44	2.75	-	1.07	0.90	1.44	1.49
$P_{11}(-)$	1694	41	2.6	-	1.13	0.92	1.18	1.41
P_{13}	1728	72	2.45	4.5	1.02	0.93	1.47	1.37
S_{11}	1696	31	0.77	-	1.11	1.10	1.42	1.52
$S_{11}(\omega p)$	-	-	-	-	1.12	0.94	1.40	1.52

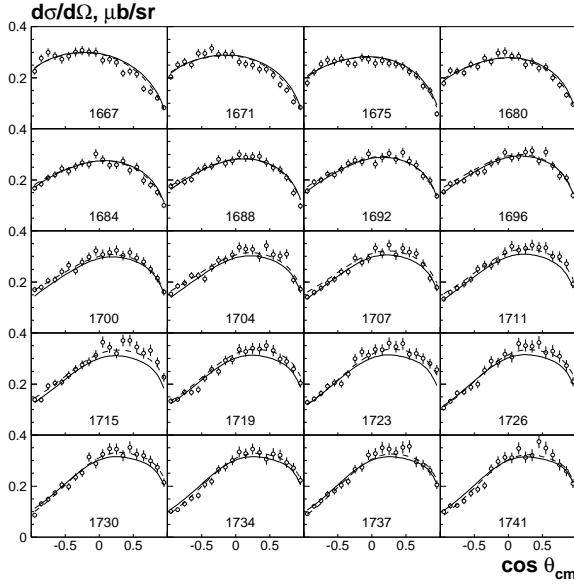


Figure 1: Differential cross section $\gamma p \rightarrow \eta p$ in the mass region 1660-1750 MeV [25] taken from the Durham data base. The full curves correspond to the solution BG2010-02M and the dashed curves to the solution $P_{11}(+)$. Errors for experimental points are taken as square root from sum of statistic and systematic errors.

The systematic deviations between data and fit show that our solutions miss some physics in this region. The missing contribution is likely either in S or P wave. A contribution either from the D or F partial waves provides a complicated angular behavior, which is not compatible with the smooth observed angular distributions.

The most striking explanation of this phenomenon is the existence of a narrow state with the mass around 1700 MeV. Indeed, including a narrow state significantly improves the description of the $\gamma p \rightarrow \eta p$ data in this mass region. Starting from the solution BG2010-02M and assuming the contribution of a narrow state,

we have found four solutions which provided a similar χ^2 : two solutions with a P_{11} narrow state, one solution with a narrow state in the P_{13} partial wave and one solution with a narrow S_{11} resonance. In Table 1 our solutions are listed; for each solution we give the total χ^2 , the χ^2_{sel} for the data from Ref. [25] in the energy interval of 1660 – 1750 MeV, and the χ^2_{Σ} for the data on beam spin asymmetry from Refs. [23, 24] and from Ref. [36].

The two solutions with a narrow P_{11} resonance differ by the interference of this state with other partial waves. For positive interference (solution $P_{11}(+)$), the mass of the resonance optimizes at 1719 MeV, and the width at 44 MeV. The solution exhibits a clear peak at 1719 MeV where the experimental total cross section reaches its maximum. The solution with negative interference (solution $P_{11}(-)$) describes better the region around 1690 MeV where the total cross section reaches the minimum. In this solution the mass optimizes for 1694, the width for 41 MeV (see Table 1). The differential cross section, the solution BG2010-02M without a resonance, and the solution with $P_{11}(+)$ resonance are shown in Fig. 1; the total cross section in this mass region calculated from experimental data points is compared with solution BG2010-02M and both P_{11} solutions in Fig. 2a. Although the solution with positive interference reproduces better the total cross section, the χ^2_{sel} for the fit to the differential cross section is practically the same.

Indeed, the $P_{11}(+)$ solution solves the problem in the description of the differential cross section in the forward angular region, but slightly exceeds the differential cross section in the backward region (see mass bins 1707, 1711 and 1715 MeV). The obtained values of the photo-couplings (see Table I) in both solutions are in a good agreement with estimates from Refs. [23, 24, 26] and are about 5 times smaller than the corresponding coupling for the neutron obtained in Ref. [20] from the

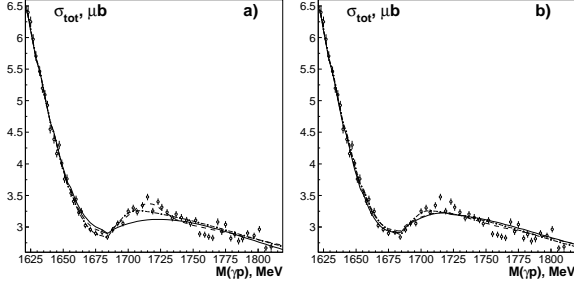


Figure 2: Comparison of the total cross section $\gamma p \rightarrow \eta p$ calculated from the data [25] with found solutions. a) The full curve corresponds to the solution BG2010-02M, the dashed curve to the solution $P_{11}(+)$ and dashed-dotted curve to the solution $P_{11}(-)$. b) The full curve corresponds to the solution BG2010-02M with ωp channel included, the dashed curve to the solution with the P_{13} narrow state and dashed-dotted curve to the solution with the S_{11} narrow state.

analysis of the GRAAL data [9, 10].

In the case of a P_{13} narrow state, a notable improvement in the description was obtained from a fit with $A_{3/2}^p \sim 2A_{1/2}^p$ and destructive interference with the other parts of the P_{13} wave. The total cross section for this solution is shown in Fig. 2. The mass of the P_{13} state optimized at 1728 MeV and width at 72 MeV. This state is relatively broader than the narrow states in other solutions and produces a rather complicated interference with the rest of the P_{13} wave. The structure, if confirmed, might be related to the anomaly in the P_{13} wave reported by CLAS in electro-production of $\pi^+\pi^-$ pairs [37].

A narrow S_{11} state only slightly improves the description of the data in the 1660-1750 MeV region. Only one solution with destructive interference with the remaining S_{11} partial wave was found. The mass of this state optimized at $M = 1685$ MeV and $\Gamma = 30$ MeV. The comparison of the experimental total cross section and the result of the fit is shown in Fig. 2b. The value $\sqrt{\text{Br}_\eta N} A_{1/2}^p$ for this solution is about 4 times smaller than that for other solutions. There is no surprise here: this resonance interferes with the largest partial wave and a small coupling can produce a notable effect.

Another - more conventional - possibility to reproduce the narrow structure is a contribution from the ωp threshold. It is known that diffractive ω production is important; possibly, its effect (due to pion exchange) is experienced already in the threshold region. The ωp channel opens at 1720 MeV. Sizable effects can be expected when ω and proton are in relative S wave. This translates into S_{11} and D_{13} partial waves. It is interesting to investigate whether the opening of this channel can explain the structure observed in [25]. To check

this assumption we introduced the ωp channel in the K-matrix parameterization of the S_{11} partial wave and fitted the couplings of the K-matrix poles and for non-resonant transition $\gamma p \rightarrow \omega p$ as free parameters. The 650-1750 MeV mass region of the MAMI data is now described better than in the fit with a narrow S_{11} resonance. The χ^2 s for this fit are given in Table 1. The description of the beam asymmetry data [23, 24] and [36] practically can not be distinguished from that obtained with the BG2010-02M solution and is not shown. The inclusion of the ωp channel in the D_{13} wave did not improve the description of the data.

The optimum strength for the non-resonant transition term $\gamma p \rightarrow \omega p$ in the S_{11} wave was found at a rather large value. However, there is a large correlation between the parameter representing the non-resonant transition amplitude and the parameters representing decays of the two $N(1535)S_{11}$ and $N(1650)S_{11}$ resonances into $p\omega$, and the resonant and non-resonant contributions cannot be distinguished on the basis of the data used here. The ωp parameters can likely be fixed when data on $\gamma p \rightarrow \omega p$ are included in the data base. This option is not yet included in our fitting program. We note that the effects of the $K\Lambda$ and $K\Sigma$ thresholds are included in our analysis automatically: the KY photo and pion induced data are an important part of our couple channel analysis. In our present solutions we do not observe a significant effects from the KY thresholds on the η photoproduction data.

Polarization observables are very useful to decide to which partial wave the structure in MAMI data can be related. Polarization measurements - including the GRAAL data on beam asymmetry for η photoproduction [36] are, of course, part of our data base. Yet, the beam asymmetry results of [23, 24] - from an alternative analysis of a limited sample of the same data and published by part of the GRAAL collaboration only - was not included. However, as mentioned above, additional evidence for a narrow state with mass around 1685 MeV was reported from the analysis of this data [23, 24] and therefore we included this data set with a relatively small weight in the present data base. The description of the MAMI data appeared to be hardly sensitive to inclusion of these data. Only the solution $P_{11}(-)$ produced a better description of the beam asymmetry data [23, 24] and even a slightly better ($\delta\chi = 0.03$) description of the MAMI data in the mass region 1650-1750 MeV. The χ^2 for the description of the MAMI data in the total mass region, in the region of 1660-1750 MeV and for the beam asymmetry data are given in Table 1. The description of the beam asymmetry data for three solutions (BG2010-02M, $P_{11}(+)$ and $P_{11}(-)$)

is shown in Fig. 3. The solutions with the P_{13} and S_{11} narrow states shows only very small deviations from the solution BG2010-02M.

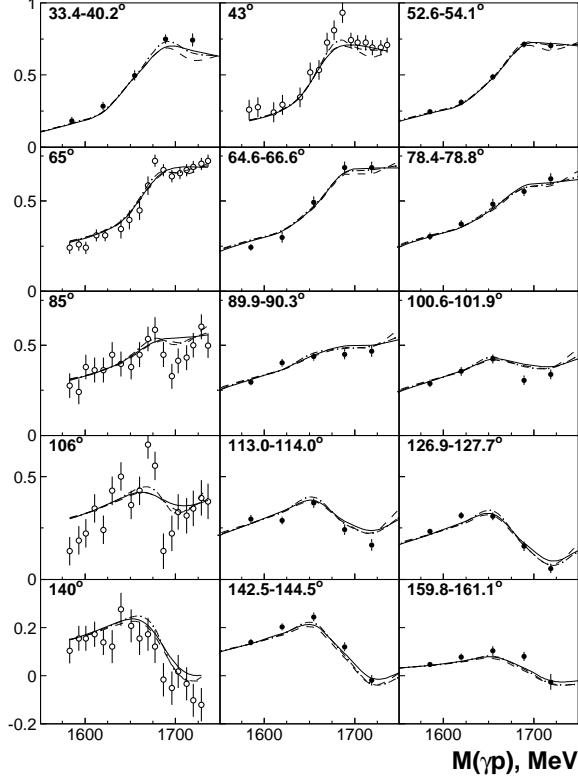


Figure 3: The description of the beam asymmetry data (shown at fixed angles) with our solutions. The open circles represent the data from [23, 24] and full circles the data from [36]. The center values of angular bins for [36] depend on the energy and are given as intervals (from the lowest energy to highest one). The full curve corresponds to the solution BG2010-02M, dashed curve to the $P_{11}(+)$ solution and dashed-dotted curve to the $P_{11}(-)$ solution.

The beam asymmetry data can hardly distinguish between the different solutions. At present, the beam asymmetry from [23, 24] might slightly favor the solution $P_{11}(-)$ but the statistical significance does not enforce one of the solutions. Future precise measurements of polarization observables are needed to decide which of the solutions proposed here corresponds best to reality.

One of the most sensitive observables which would be able to distinguish between the four solutions is the target asymmetry. The prediction of this observable from our four solutions (with ωp channel introduced in the S_{11} wave, with the narrow P_{11} states and with the narrow P_{13} state) is shown in Fig. 4. Another interesting polarization observable sensitive to these different solu-

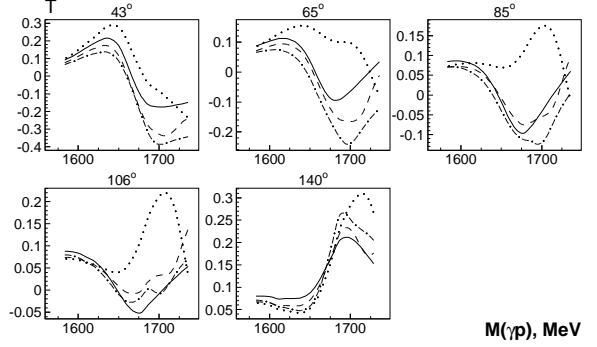


Figure 4: Prediction of the target asymmetry for η photoproduction. The full curves correspond to the solution with ωp channel included to the S_{11} partial wave, dashed curves to the $P_{11}(+)$ solution, dashed-dotted curves to the $P_{11}(-)$ solution and dotted curves to the P_{13} solution.

tions can be extracted from an experiment with a transversely polarized target and circularly polarized beam. The prediction of the so-called F -observable from the four solutions discussed above is shown in Fig. 5. With such data, even solutions with negative and positive interference between a narrow P_{11} resonance and the remaining wave could be separated if the narrow state would indeed contribute to the data.

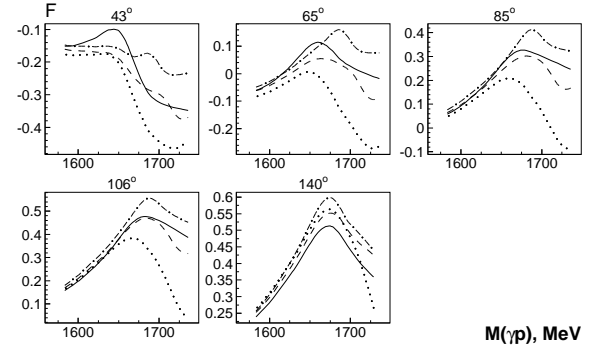


Figure 5: Prediction for the F -observable in the η photoproduction. The full curves correspond to the solution with ωp channel included to the S_{11} partial wave, dashed curves to the $P_{11}(+)$ solution, dashed-dotted curves to the $P_{11}(-)$ solution and dotted curves to the P_{13} solution.

We conclude that the new high precision data on $\gamma p \rightarrow \eta p$ cross section of Ref. [25] reveal an interesting structure in the mass region of 1660-1750 MeV. The relatively smooth angular distributions suggest that this structure can be interpreted within the P or S waves. The threshold of the ωp channel may effect the data and may contribute by a coupling of the two S_{11} resonances to ωp and by a non-resonant $\gamma p \rightarrow p\omega$ transition strength. A good fit of the data is achieved when the ωp

channel is included even though the fit is unable to decide which of the two mechanisms is more important. Assigning the effect to the P -wave, the data can be explained only with introduction of a narrow resonance, in particular when the data [23, 24] on the beam asymmetry Σ are included. A narrow P_{11} resonance - interfering destructively within the P_{11} wave - would be preferred in this case.

High statistic polarization data on target asymmetry and on the double polarization variable F should provide the necessary constraints to define which partial wave is responsible for the structure observed in mass region of 1660-1750 MeV in the $p\eta$ cross section. In the end it may provide the information needed to decide whether or not a narrow baryon resonance exists in this mass range.

The work has been supported by the DFG within SFB/TR16. M.V.P. is thankful to N. Sverdlova for comments on the text and to I. Strakovsky for correspondence.

References

- [1] K. Nakamura *et al.* [Particle Data Group], J. Phys. G **37** (2010) 075021.
- [2] E. Klempt and J. M. Richard, Rev. Mod. Phys. **82** (2010) 1095.
- [3] D. Diakonov, V. Petrov and M. V. Polyakov, Z. Phys. A **359** (1997) 305.
- [4] D. Diakonov and V. Petrov, Phys. Rev. D **69** (2004) 094011.
- [5] R. A. Arndt *et al.*, Phys. Rev. C **69**, 035208 (2004).
- [6] J. R. Ellis, M. Karliner and M. Praszalowicz, JHEP **0405** (2004) 002;
M. Praszalowicz, Acta Phys. Polon. B **35** (2004) 1625.
- [7] I. G. Alekseev *et al.* [EPECUR Collaboration], AIP Conf. Proc. **1056** (2008) 396.
- [8] M. V. Polyakov and A. Rathke, Eur. Phys. J. A **18**, 691 (2003).
- [9] V. Kuznetsov [GRAAL Collaboration], arXiv:hep-ex/0409032.
- [10] V. Kuznetsov *et al.*, Phys. Lett. B **647**, 23 (2007).
- [11] I. Jaegle *et al.* [CBELSA Collaboration and TAPS Collaboration], Phys. Rev. Lett. **100** (2008) 252002.
- [12] I. Jaegle *et al.*, Eur. Phys. J. A **47**, 89 (2011)
- [13] F. Miyahara *et al.*, Prog. Theor. Phys. Suppl. **168**, 90 (2007).
- [14] D. Werthmuller [for the Crystal Ball/TAPS collaborations], Chin. Phys. C **33**, 1345 (2009).
- [15] A. V. Anisovich, I. Jaegle, E. Klempt, B. Krusche, V. A. Nikonov, A. V. Sarantsev and U. Thoma, Eur. Phys. J. A **41** (2009) 13
- [16] V. Shklyar, H. Lenske, U. Mosel, Phys. Lett. **B650**, 172-178 (2007).
- [17] R. Shyam, O. Scholten, Phys. Rev. **C78**, 065201 (2008).
- [18] X. H. Zhong and Q. Zhao, arXiv:1106.2892 [nucl-th].
- [19] M. Doring and K. Nakayama, Phys. Lett. B **683** (2010) 145 [arXiv:0909.3538 [nucl-th]].
- [20] Y. I. Azimov, *et al.*, Eur. Phys. J. A **25**, 325 (2005) [arXiv:hep-ph/0506236].
- [21] A. Fix, L. Tiator and M. V. Polyakov, Eur. Phys. J. A **32**, 311 (2007) [arXiv:nucl-th/0702034].
- [22] V. Kuznetsov *et al.*, Phys. Rev. C **83** (2011) 022201(R).
- [23] V. Kuznetsov *et al.*, Acta Phys. Polon. B **39**, 1949 (2008);
V. Kuznetsov, *et al.*, arXiv:hep-ex/0703003.
- [24] V. Kuznetsov and M. V. Polyakov, JETP Lett. **88**, 347 (2008).
- [25] E. F. McNicoll *et al.* [Crystal Ball Collaboration at MAMI], Phys. Rev. C **82** (2010) 035208.
- [26] V. Kuznetsov, M. V. Polyakov and M. Thurmman, arXiv:1102.5209 [hep-ph].
- [27] A. Anisovich, E. Klempt, A. Sarantsev and U. Thoma, Eur. Phys. J. A **24**, 111 (2005).
- [28] E. Klempt, A. V. Anisovich, V. A. Nikonov, A. V. Sarantsev and U. Thoma, Eur. Phys. J. A **29** (2006) 307.
- [29] A. V. Anisovich and A. V. Sarantsev, Eur. Phys. J. A **30**, 427 (2006).
- [30] A. V. Anisovich *et al.*, Eur. Phys. J. A **34** (2007) 129.
- [31] A. V. Anisovich *et al.*, Eur. Phys. J. A **25**, 427 (2005).
- [32] A. V. Anisovich *et al.*, Eur. Phys. J. A **47** (2011) 27.
- [33] Bonn-Gatchina partial wave analysis. http://partial_wave_analysis.hiskp.uni-bonn.de/
- [34] B. Krusche *et al.*, Phys. Rev. Lett. **74**, 3736 (1995).
- [35] V. Crede *et al.*, Phys. Rev. C **80**, 055202 (2009).
- [36] O. Bartalini *et al.*, Eur. Phys. J. A **33**, 169 (2007).
- [37] M. Ripani *et al.* [CLAS Collaboration], Phys. Rev. Lett. **91**, 022002 (2003).